Double photoionization of He at 80 eV excess energy in the equal-energy-sharing condition

G. Turri,[1,2,*] L. Avaldi,[3] P. Bolognesi,[3] R. Camilloni,[3] M. Coreno,[2] J. Berakdar,[4] A. S. Kheifets,[5] and G. Stefani[6]
[1]*Dipartimento di Fisica, Politecnico di Milano, Milano, Italy*
[2]*INFM, Laboratorio TASC, Area Science Park, Basovizza, Trieste, Italy*
[3]*CNR-IMAI, Area della Ricerca di Roma, Casella Postale 10, 00016 Monterotondo Scalo, Italy*
[4]*Max Planck Institut für Mikrostrukturphysik, Weinberg 2, 06120 Halle, Germany*
[5]*Research School of Physical Science and Engineering, Australian National University, Canberra, Australian Capital Territory 2000, Australia*
[6]*Dipartimento di Fisica "E. Amaldi" and INFM Unità di Roma III, Università di Roma Tre, Via della Vasca Navale, Roma, Italy*
(Received 7 August 2001; published 4 February 2002)

The high flux of the gas-phase beamline at the Elettra storage ring, Trieste (Italy), and the efficiency of a multicoincidence end station have been combined to measure the triple-differential cross section (TDCS) for the double photoionization (DPI) of He at excess energies $E=20$ and 80 eV. The TDCS has been measured in the equal-energy-sharing kinematics, in which the kinetic energies of the two photoelectrons are equal ($E_1=E_2=E/2$). The experiments are compared with the predictions of a many-body Coulomb wave method and a convergent close-coupling calculation. The symmetrized gerade amplitudes of the He (DPI) extracted by the experiments as well as by the two calculations have been fitted by a Gaussian function. The results support the validity of the parametrization of the gerade amplitude via only one parameter, the full width at half maximum $\vartheta_{1/2}$, of the Gaussian function, up to 80 eV above threshold.

DOI: 10.1103/PhysRevA.65.034702 PACS number(s): 32.80.Fb

The double photoionization (DPI) of He represents the archetype of the three-body problem (two interacting electrons coupled to a positive *structureless* residual ion). The complete characterization of the process implies the detection of the two photoelectrons in coincidence after energy and angular selection. In such an experiment the triply differential cross section $d^3\sigma/d\Omega_1 d\Omega_2 dE_1$ (TDCS), i.e., a cross section differential in the angles of emission of the two photoelectrons $\Omega_1=(\vartheta_1,\varphi_1)$ and $\Omega_2=(\vartheta_2,\varphi_2)$ and in one kinetic energy, is measured. The kinetic energy E_2 of the other electron is determined by energy conservation $h\nu\text{-}V(\mathrm{He}^{2+})=E=E_1+E_2$, where $V(\mathrm{He}^{2+})=79.004$ eV is the He double-ionization potential [1] and E is the excess energy. In an alternative experimental approach the TDCS can also be obtained by detecting in coincidence the He^{2+} recoil ion and one of the two photoelectrons, as in the COLTRIMS method [2]. The value of the total DPI cross section for He ($\cong 8.76\times10^{-21}$ and 3.83×10^{-21} cm^2 at 20 and 80 eV above threshold, respectively [3]), the need of an energetic and tunable photon source, and the intrinsic difficulties of coincidence experiments have hampered the measurements of the TDCS for a long time. The first experimental measurement of the He TDCS was performed by Schwarzkopft *et al.* [4] at $E=20$ eV in the equal-energy-sharing condition ($E_1=E_2=E/2$). Since then several measurements have been reported in the literature (see Briggs and Schmidt [5] for a review of the data up to 2000 and Kheifets and Bray [6] for more recent data). On the theoretical side, considerable progress has been made in the last few years in the description of the three-body Coulomb problem; however, a universally applicable theory is still missing. Experimentally, at a fixed incident energy the TDCS can be measured under a variety of kinematic conditions (changing the energy sharing between the electrons and/or their angles of emission). This results in a large body of data and hampers direct comparisons among different sets of data and between experiment and theory.

By considering the invariance with respect to rotation around the electric-vector direction of the incident radiation and the general properties of the spherical harmonics, the TDCS can be separated into geometrical factors and dynamical parameters [7]. This leads to a form of the TDCS that in the case of incident radiation that propagates along the $\mathbf{z}$ axis and is fully linearly polarized along the $\boldsymbol{\varepsilon}=\varepsilon\mathbf{x}$ axis can be written as [7]

$$\frac{d^3\sigma}{d\Omega_1 d\Omega_2 dE_1}\propto|a_g(E_1,E_2,\vartheta_{12})(\cos\vartheta_1+\cos\vartheta_2) + a_u(E_1,E_2,\vartheta_{12})(\cos\vartheta_1-\cos\vartheta_2)|^2, \tag{1}$$

where ϑ_1 and ϑ_2 are the angles of emission of the two photoelectrons with respect to $\boldsymbol{\varepsilon}$ and ϑ_{12} is the angle between the directions of emission of the two photoelectrons. The complex amplitudes a_g and a_u are, respectively, symmetric and antisymmetric relative to the exchange of E_1 and E_2. The ϑ_{12} and E dependence of these amplitudes includes all the physical information on the dynamics of the process, i.e., the effects of the electron-electron and electron–residual-ion interactions. Thus it is of considerable interest to find a suitable representation of these amplitudes that may facilitate comparisons across a variety of reaction kinematics [6,8–10].

In the case of equal-energy-sharing experiments $a_u=0$; thus the TDCS reduces to a simple form. Since the first mea-

*Present address: Western Michigan University and Lawrence Berkeley National Laboratory, ALS Division, 1 Cyclotron Road MS 7-222 Berkeley, CA 94720.

surements of the TDCS the symmetric amplitude a_g, often called in the literature the ''correlation factor,'' has been represented by a Gaussian function,

$$a_g \propto \exp[-2\ln 2(\vartheta_{12}-180)^2/\vartheta_{1/2}^2], \quad (2)$$

where $\vartheta_{1/2}$ is the correlation width. This form follows from the Wannier-type theories [11,12] in which the angular variation near the Wannier saddle decouples from the radial motion [13] and can be described by the ground-state wave function of a harmonic oscillator. These models are expected to be valid only at small excess energies. However, it turned out that the Gaussian form may be used as a useful approximation to describe several experiments at higher excess energy [10]. More recently Kheifets and Bray [6] supported the validity of the Gaussian parametrization via a fully numerical calculation in the range of excess energy 3–80 eV.

The measurement of the TDCS in equal energy sharing becomes increasingly difficult as E increases. Indeed, the total DPI cross section rises from threshold up to its maximum value at $E=20$ eV and then rapidly decreases [3]. Moreover, the equal-energy-sharing kinematic condition corresponds to the minimum of the energy distribution $d\sigma/dE_1$ (see, for example, Fig. 7 in [5]). By taking advantage of the high flux of the Gas-phase photoemission beamline at the Elettra storage ring and the efficiency of the multicoincidence end station [14], we have measured the TDCS of He in the equal-energy-sharing condition at $E=80$ eV. These measurements extend the studies of He DPI in equal energy sharing, so far limited to $E=60$ eV [15], to a higher excess energy.

The gas-phase photoemission beamline and the end station have been described in detail elsewhere [14,16,17]. The multicoincidence experimental chamber is equipped with ten electrostatic analyzers. Seven analyzers are mounted on a turntable that rotates in the plane perpendicular to the direction **z** of propagation of the incident radiation. The remaining three analyzers are mounted on a smaller turntable at 0°, 30°, and 60°, respectively, with respect to the polarization vector $\boldsymbol{\varepsilon}$ of the light.

In the present experiments the measurements were performed in the plane perpendicular to the direction of the incident beam. Each analyzer was operated with an energy resolution of 0.3 and 1.2 eV at $E=20$ and 80 eV, respectively, and with an angular acceptance of $\pm 3°$. The coincidence angular distributions are measured by selecting electrons ejected at fixed directions with the three analyzers on the smaller turntable and for successive rotations of the larger turntable. Up to 21 coincidence pairs are obtained simultaneously. In the following the electron measured at a fixed direction will always be labeled ''1.'' Two sets of measurements at $E=20$ and 80 eV were performed. Several results in equal-energy-sharing conditions have been reported in the literature at $E=20$ eV [4,9,18–21]. Thus the measurement at $E=20$ eV was used as a benchmark for the behavior of the spectrometer.

The relative efficiency of the analyzers was calibrated via the measurement of photoelectron angular distributions with known β parameters [Ne($2p$) and Ar($3p$) at 10 and 40 eV above threshold, respectively] and then confirmed by determining the β parameter of the photoelectron angular distribution of He($1s$) at the same kinetic energies. The overlap of the field of view of the analyzers was checked by a series of photoemission measurements at different relative positions of the incident beam and the full spectrometer. Then the efficiency correction derived from the noncoincidence measurements was applied to the coincidence ones. The validity of this assumption was tested by measuring the coincidence yield at two positions of the larger turntable that allow overlap of two nearby analyzers. Therefore all the experimental data are internormalized and can be reported on the same relative scale. This can be checked by observing that the same coincidence yield is measured for different configurations of the analyzers corresponding to the same kinematics [for example ($\vartheta_1=0°$ and $\vartheta_2=120°$, 150°, and 180°) and ($\vartheta_1=0°$, 30°, and 60° and $\vartheta_2=180°$)].

The experiments were performed at $h\nu=99$ and 159 eV using the first harmonic of the undulator. The photoelectron angular distribution of He($1s$) at these photon energies confirmed that within the uncertainty of the measurements the incident radiation is fully linearly polarized along the **x** axis. With a photon flux of 1.4×10^{12} photon/s (measured by an IRS photodiode placed behind the end station) and a residual pressure in the chamber of about 7×10^{-5} Torr the coincidence count rate at $E=80$ eV was about 10 mHz per pair of detectors and the true-to-random ratio always better than 10. The total acquisition time in the case of the measurements at $E=80$ eV was $\approx$13 h.

The TDCSs measured at $E=20$ and 80 eV are reported in Figs. 1(a) and 1(b), respectively. The experiments are compared with the predictions of the convergent close-coupling theory (CCC) theory [22,23] and the three-body Coulomb wave method including virtual states (VS-3C) [24,25].

The CCC method is a fully numerical approach and relies on intensive computation. For the final state it solves the Schrödinger equation for the system of a photoelectron scattering on the He^+ ion by employing the close-coupling expansion of the total wave function. The DPI results from the electron-impact ionization of the He^+ ion. The initial state is represented by a highly correlated Hylleraas-type wave function. The CCC integrated DPI cross sections agree with the experiments over a broad energy range [26]. The use of a highly correlated ground-state wave function ensures that the results have insignificant dependence on the three gauges. Therefore only the velocity gauge calculation is shown in Figs. 1(a) and 1(b).

In the VS-3C method [25] the three-body Hilbert space is subdivided into two regions. In the ''inner'' or ''short-range'' region in which the potential energy (U) dominates over the kinetic energy (K), the two electrons occupy all the virtual states off the two-body energy shell, while conserving the total energy. In the ''far zone,'' where the asymptotic regime ($K>U$) is reached, the virtual states are matched smoothly to the well-known 3C wave function [24] to achieve correct asymptotic behavior. For the initial state a correlated wave function that fulfills the cusp condition has been adopted. In all cases considered so far [25], the VS-3C calculations turned out to be gauge dependent, but not as strongly as when using the 3C model. In particular, the calculations per-

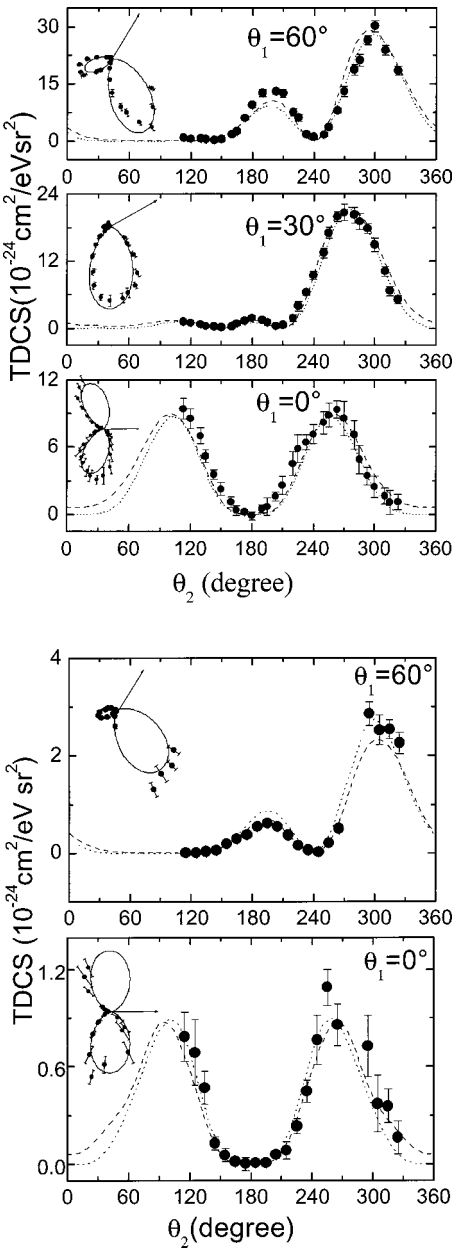

FIG. 1. He TDCSs for $E=20$ eV, $E_1=E_2=10$ eV (a) and $E=80$ eV, $E_1=E_2=40$ eV (b). The experimental TDCSs are compared with the predictions of the CCC (dashed lines) and VS-3C (dotted line) models in the velocity form. In the top left corner of each panel the experimental TDCSs are reported also in polar plots and compared with the results of the fit using Eq. (1) with the amplitude represented by the Gaussian function in Eq. (2).

formed with the VS-3C method the length and velocity form differ mainly in magnitude, but less in shape. This is the case for the results presented in this paper and hence we show only the cross sections evaluated in the velocity form. The VS-3C calculations are in general in better agreement with the experimental data than calculations based on the 3C wave function only. The latter are not presented here for the sake of clarity of figures. Both the experiments and the VS-3C calculation have been normalized to the CCC calculation at $\vartheta_1=0°$ and $\vartheta_2=240°$ and 265° at $E=20$ and 80 eV, respectively. An acceptable agreement between theories and experiments in both shape and relative intensity is observed for the three measured TDCSs at $E=20$ eV. Similar agreement is observed at $E=80$ eV, although it appears that a slightly different relative intensity is predicted by the two theories when ϑ_1 changes from 0° to 60°. In the top left corner of each panel the experimental data are reported in polar plots and compared with the results of a fit based on the Gaussian ansatz [11,12] for the a_g amplitude. For each excess energy the fit to the full set of measured TDCSs depends only on two parameters: a scaling factor and the correlation width $\vartheta_{1/2}$, which appears in Eq. (2). The best values for the correlation widths are 90 ± 3 and 120 ± 4 for $E=20$ and 80 eV, respectively. The value obtained at $E=20$ eV is in good agreement with the results of previous measurements collected in Table I. This rules out major experimental artifacts in the measurements of the present TDCS.

TABLE I. The $\vartheta_{1/2}$ values of the Gaussian function fitted to different sets of experimental data at $E=20$ eV.

Ref. [4]	90.4 ± 4
Ref. [18]	90.9 ± 2
Ref. [9][a]	91 ± 2
Ref. [19]	91.6 ± 2
Ref. [20]	90.2 ± 2
Ref. [21]	91 ± 3
Present work	90 ± 3

[a]In this case $E=18.6$ eV.

The main information on the reaction mechanism and many-electron correlations is contained in the amplitude a_g. The $|a_g|^2$ extracted from the TDCSs calculated by the two models are compared with the experimental ones and with

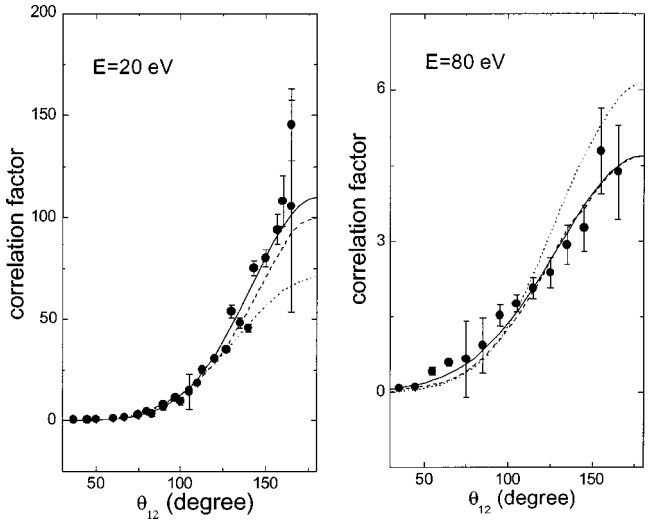

FIG. 2. $|a_g|^2$ extracted from the experimental data compared with the ones predicted by the CCC (dashed line) and VS-3C (dotted line) models. The full line is the best fit to the experimental data of a Gaussian function with $\vartheta_{1/2}=90\pm3$ and 120 ± 4 for $E=20$ and 80 eV, respectively.

TABLE II. The $\vartheta_{1/2}$ values of the Gaussian function fitted to the present experimental data and to the theoretical amplitudes.

	E	
	20 eV	80 eV
Experiment	90 ± 3	120 ± 4
CCC	90.6	117
VS-3C	103	108

the Gaussian functions that provide the best fit to the experiments in Fig. 2. At the ϑ_{12} values where multiple experimental determinations exist a weighted average has been calculated and reported in Fig. 2. Only data relative to $\vartheta_{12} \leqslant 170°$ have been represented. The amplitudes extracted by the CCC calculations are in fair agreement with the experiments, while the ones derived by the VS-3C model seem to predict a less correlated electron motion at $E=20$ eV and a more correlated one at $E=80$ eV. This is clearly indicated by the values of $\vartheta_{1/2}$ obtained by a fit with a Gaussian function to the theoretical amplitudes and reported in Table II. These results show that the use of the amplitude makes the comparison among experiments and theory more compact and direct, and allows one to outline differences among the theoretical predictions that may be hidden in the comparison of the TDCSs because of the modulation imposed by the kinematical factor.

In conclusion, we have extended the measurements of the TDCS of He in equal-energy-sharing conditions up to $E=80$ eV. We have shown that an efficient comparison between experiment and theory can be achieved using $|a_g|^2$ instead of the TDCS. Moreover, the Gaussian ansatz appears to be a suitable representation of the a_g amplitude up to this energy. This confirms the numerical results of Kheifets and Bray [6]. The Gaussian representation of the a_g amplitude is a very useful tool to reduce the comparison among different experiments and experiments and theory to only one parameter: the value of $\vartheta_{1/2}$. Whether the use of the Gaussian ansatz might be extended to higher excess energy, where the motion in the continuum of the two electrons is expected to become less correlated, is still a matter of investigation.

This work was partially supported by the INFM Progetto Luce di Sincrotrone (Application No. GAPH002S01). The authors are grateful to the staff of the gas-phase beamline at Elettra for their support.

[1] D. B. Thompson *et al.*, J. Phys. B **31**, 2225 (1998).
[2] J. Ullrich *et al.*, J. Phys. B **30**, 2917 (1997).
[3] J. A. R. Samson, W. C. Stolte, Z. X. He, J. N. Cutler, Y. Lu, and R. J. Bartlett, Phys. Rev. A **57**, 1906 (1998).
[4] O. Schwarzkopf, B. Krässig, J. Elminger, and V. Schmidt, Phys. Rev. Lett. **70**, 3008 (1993).
[5] J. Briggs and V. Schmidt, J. Phys. B **33**, R1 (2000).
[6] A. S. Kheifets and I. Bray (unpublished).
[7] A. Huetz, P. Selles, D. Waymel, and J. Mazeau, J. Phys. B **24**, 1917 (1991).
[8] L. Malegat, P. Selles, and H. Huetz, J. Phys. B **30**, 251 (1997).
[9] L. Malegat *et al.*, J. Phys. B **30**, 263 (1997).
[10] S. Cvejanovic and T. J. Reddish, J. Phys. B **33**, 251 (2000).
[11] A. R. P. Rau, J. Phys. B **9**, L283 (1976).
[12] J. M. Feagin, J. Phys. B **17**, 2433 (1984).
[13] J. M. Rost, J. Phys. B **27**, 5923 (1994).
[14] R. R. Blyth *et al.*, J. Electron Spectrosc. Relat. Phenom. **101-103**, 959 (1999).
[15] C. Dawson *et al.*, J. Phys. B **34**, L525 (2001).
[16] P. Melpignano, S. DiFonzo, A. Bianco, and W. Jark, Rev. Sci. Instrum. **66**, 2125 (1995).
[17] P. Bolognesi *et al.*, J. Phys. B **34**, 3193 (2001).
[18] O. Schwarzkopf and V. Schmidt, J. Phys. B **28**, 2847 (1995).
[19] R. Dörner *et al.*, Phys. Rev. A **57**, 1074 (1993).
[20] H. Bräuning *et al.*, J. Phys. B **31**, 5149 (1998).
[21] J. P. Wightman, S. Cvejanovic, and T. J. Reddish, J. Phys. B **31**, 1753 (1998).
[22] A. S. Kheifets and I. Bray, J. Phys. B **31**, L447 (1998).
[23] A. S. Kheifets and I. Bray, Phys. Rev. Lett. **81**, 4588 (1998).
[24] M. Brauner, J. S. Briggs, and H. Klar, J. Phys. B **22**, 2265 (1989).
[25] I. Berakdar, Phys. Rev. Lett. **78**, 2712 (1997).
[26] A. S. Kheifets and I. Bray, Phys. Rev. A **58**, 4501 (1998).